70th International Astronautical Congress (IAC), Washington D.C., United States, 21-25 October 2019.

IAC-19-C2.IP.10.x50161

The beneficiation of lunar regolith using electrostatic separation for Space Resource Utilisation

J.N. Rasera[a,b,*], J.J. Cilliers[a], J.-A. Lamamy[b], K. Hadler[a]

[a] *Department of Earth Science and Engineering, Imperial College London, Exhibition Road, London, SW7 2AZ*, United Kingdom j.rasera@imperial.ac.uk; j.j.cilliers@imperial.ac.uk; k.hadler@imperial.ac.uk
[b] *ispace Europe SA, rue de l'Industrie 5, Luxembourg City, L-1740, Luxembourg*, j-rasera@ispace-inc.com; j-lamamy@ispace-inc.com
* Corresponding Author

Abstract

Differences in the electrostatic properties of materials can be exploited for both the sizing and enrichment of minerals. In this study, the motion of silica particles falling through an electrostatic field was investigated to characterise a custom free-fall electrostatic separator. The motion was affected by varying the magnitude of the electrostatic field and the spacing of the electrodes. SiLibeads (spherical silica) were sized and tribocharged in a borosilicate glass beaker and fed into the separator. Fourteen electrostatic field strengths each generated at three different electrode spacings (75 mm, 150 mm, and 225 mm) were studied. The percentage of particles reporting to each electrode was measured.

Analyses of the results indicate that the expected linear increase in the field strength does not increase proportionally the amount of material reporting to each electrode, indicating that additional underlying parameters must be characterised. Further, an analysis of the variance between the measurements indicates that there are almost no significant effects on the separator's operation due to changing either the field strength or electrode spacing. However, two statistically unique operating conditions were identified. The measurements collected at a field strength of 0.04 kV/mm with a 75-mm spacing were unique relative to other field strengths at that spacing and may indicate an optimal operating condition. Further, the data collected at each electrode spacing with a constant electric field strength of 0.06 kV/mm were also found to be unique. This implies that there may be a performance dependence on electrode spacing in addition to the field strength. Further analysis and experimentation are required to draw more detailed conclusions.

Keywords: Lunar resources, beneficiation, electrostatic, space resource utilisation (SRU)

Nomenclature

$\overrightarrow{F_p}$	Net force on a particle, N
$\overrightarrow{F_g}$	Gravitational force, N
$\overrightarrow{F_d}$	Stokes' drag force, N
$\overrightarrow{F_{ad}}$	Adhesion force, N
$\overrightarrow{F_C}$	Coulomb force, N
m_p	Mass of a particle, kg
$\vec{g}$	Acceleration due to gravity, m/s^2
η_f	Viscosity of a fluid, kg/m·s
r_p	Radius of a particle, m
$\overrightarrow{v_p}$	Velocity of a particle, m/s
q_p	Charge on a particle, C
q_i	Charge on a nearby particle, C
ε_0	Vacuum permittivity, F/m
$\overrightarrow{R_p}$	Position of a particle, m
$\overrightarrow{R_i}$	Position of a nearby particle, m
$\vec{E}$	Electrostatic field strength, V/m

Acronyms/Abbreviations

SRU	Space Resource Utilisation
ANOVA	Analysis of Variance

1. Introduction

Space Resource Utilisation (SRU) has the potential to be the breakthrough technology that enables the further exploration and habitation of space by humankind. The use of in-space materials to provide water, fuel and building materials reduces significantly the launch mass, therefore reducing dramatically the cost of space travel. The production of oxygen on the Moon using lunar regolith is the first step for SRU, since it can be used both to sustain human life and as fuel for further exploration.

1.1 Space Mining Flowsheet

As on Earth, mining in space will necessitate a number of distinct processing steps. The sequence of these steps, and the technologies involved in them, is known as a flowsheet. Hadler et al [1] have adapted a typical terrestrial flowsheet for lunar mining, as seen in Fig. 1. The excavation and extraction steps have been studied in great detail [2,3]. The linking stage of beneficiation, however, whereby the feedstock is prepared from the lunar regolith according the

requirements of the subsequent extraction step, has been largely under-studied.

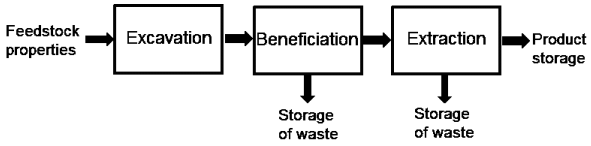

Fig. 1. Universal flowsheet for SRU processes [1].

Over 20 different reduction processes have been proposed in the literature for metal and oxygen production from lunar regolith [3]. The four main contenders being considered by NASA and ESA, however, are: Hydrogen reduction of ilmenite (<2% yield) [4]; carbothermal reduction of silicates and iron oxides (~10% yield) [5]; molten regolith electrolysis (estimated to be 20-40% yield) [6]; and, molten salt electrolysis (up to 100% yield) [7]. Of these technologies, hydrogen reduction has received the most attention, and its working principles are well-characterised.

1.2 Need for Beneficiation

As the feedstock characteristics required by hydrogen reduction processes are well-defined relative to other methods, it is considered here for illustrative purposes. One such process, patented by Gibson and Knudson [8], requires the feedstock ilmenite content to be between 80 and 90%, with a particle size ranging from 20-200 µm.

In the "high-titanium" areas of the lunar mare, ilmenite is found in the regolith at up to 20% by mass and is lower elsewhere [9]. On the Moon, 23% of the regolith is finer than 20 µm [10], making the size separation step alone appreciable in and of itself.

Furthermore, beneficiation must be considered in order to properly evaluate mine scale, as has been described in detail by Cilliers, Rasera and Hadler [11].

1.3 Electrostatic Beneficiation

The separation of regolith by size and particle type presents numerous challenges due to the high fraction of fine particles, a variety of particle shapes, the range of materials present (glasses, mineral fragments, agglutinates), and the lunar environmental constraints. On Earth, most mineral separations are carried out using water as carrier fluid, with many exploiting density differences between mineral types. A different approach is required for lunar SRU.

All beneficiation technologies separate minerals from waste using differences in physical properties (e.g., density, surface properties, electromagnetic characteristics). Electrostatic separation can be carried out by manipulating the Coulomb force. Both of these approaches have been demonstrated as effective means of separating and enriching complex mixtures of minerals [12-21]. Compared to other waterless techniques, electrostatic ones have received the greatest amount of attention for lunar SRU [22].

The aim of this study was to characterise a simple tribocharging system and free-fall electrostatic mineral separator, largely following the designs of Trigwell et al [16-18], Quinn et al [19], and Captain et al [20]. While these works have generally employed on high potential differences to generate stronger electrostatic fields (>0.4 kV/mm) in a fixed separator geometry, this work attempts to characterise simple single-component (silica) particle charging and free-fall motion in weaker fields (<0.2 kV/mm) using multiple geometries.

2. Material and Methods

Spherical silica SiLibeads (SiO_2 content ≥99.98%) were used for these experiments. Whilst silica is uncommon in the lunar regolith, uniform, spherical particles can be easily modelled and minimise uncertainty introduced by shape effects. The particles were screened down to 70-110 µm and were sized using a Malvern Panalytical Mastersizer 3000 (Fig. 2). Compared to the lunar regolith with an average size (D_{50}) of 72 µm with over 20% passing (D_{20}) below 20 µm, the silica sample was found to have a D_{50} of 87 µm and a D_{20} of 71 µm; while this is larger than the regolith (D_{50} = 72 µm [9]), smaller size fractions were found to be more strongly affected by Stokes' drag, making it challenging to characterise the free-fall separator. Future *in vacuo* testing is envisioned and will employ finer fractions.

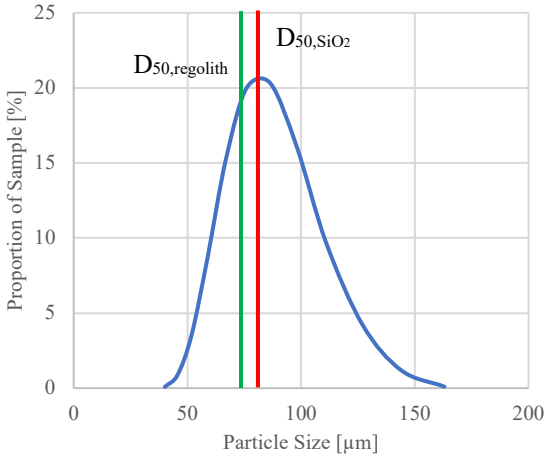

Fig. 2. Size distribution of silica particles. The D_{50} values for the sample and the lunar regolith are indicated by the red and green lines, respectively.

Tribocharging was performed by swirling 10 g of SiLibeads in a borosilicate glass beaker for 20 seconds. The charge was then measured using a Keithley 6517B electrometer and a Monroe Faraday cup. Ambient temperature and humidity in the lab were monitored using a calibrated Kane DTH10 pen digital thermohygrometer and were recorded during each test.

The free-fall separator, seen in Fig. 3, was custom-designed and built, based off of the design employed by

Trigwell et al [16-18], Quinn et al [19], and Captain et al [20]. An improvement made for this apparatus is the use of programmable FLS40 linear stages from Fuyu Technology to precisely control the position of the two 320 by 150 mm copper electrodes; the stages allow electrodes to be positioned as close as 60 mm, and up to 340 mm apart. Further, each electrode is powered by a XP Glassman FJ60-series power supply, capable of producing up to ±60 kV, greatly increasing the capacity to generate strong electrostatic fields with larger electrode spacing. These features allow for detailed investigations into the effect of field strength, electrode voltage, and symmetrical and asymmetrical electrode position, which have not been investigated holistically in the literature.

The entire apparatus is mounted inside a Faraday cage to protect against accidental discharge, and to minimise inductive interference from external sources when measuring charge. Material is fed into the chamber through a slot in the top. For this study, a borosilicate glass funnel was employed, however future studies will employ a wider range of materials and injection methods.

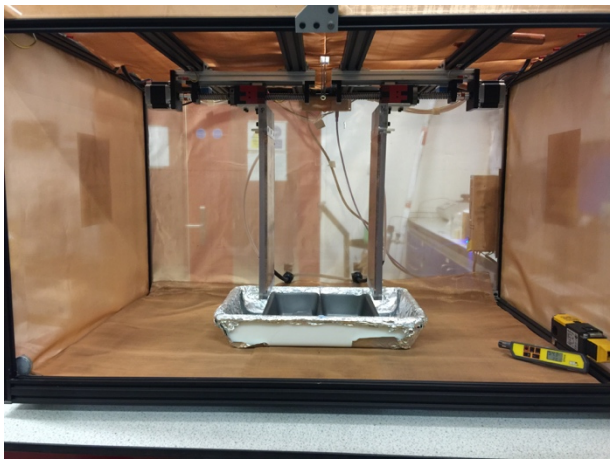

Fig. 3. Free-fall separator in the mineral processing lab at Imperial College London. Here, electrodes are spaced at 225 mm.

For these experiments, three electrode spacings were employed: 75 mm (following [16-20]), 150 mm and 225 mm. At each spacing, the voltage was varied to produce a consistent, uniform electrostatic field. The field strength ranged from 0.01 to 0.2 kV/mm, increasing by 0.01 kV/mm up to 0.1 kV/mm, then by 0.025 kV/mm up to 0.2 kV/mm. The higher-fidelity region was selected based on trends identified during initial exploratory experiments performed following the construction of the separator. Three 10-g samples of SiLibeads were tribocharged and injected into the separator at each of the electrode spacings under a constant field, and the mass of material collected in the hoppers below each electrode was measured and compared.

3. Theory and Calculation

The simplified sum of the forces acting on the particles in the separator is as follows:

$$\sum \vec{F_p} = \vec{F_g} + \vec{F_d} + \vec{F_{ad}} + \vec{F_C} \quad (1)$$

$$\sum \vec{F_p} = m_p\vec{g} + 6\pi\eta_f r_p \vec{v_p} + \frac{q_p}{4\pi\varepsilon_0}\sum_{i=1}^{n} \frac{q_i(\vec{R_p}-\vec{R_i})}{|\vec{R_p}-\vec{R_i}|^3} + q_p\vec{E} \quad (2)$$

While other forces, such as buoyancy and van der Waals, do contribute to the balance, as described by Rasera et al [22], their relative contributions are orders of magnitude lower, and thus have been excluded here for simplicity. On the Moon, of course, Stokes' drag would not contribute to the balance.

Figure 4 shows the force balance acting on a spherical particle in a free-fall separator. Through the manipulation of the relative magnitudes of these forces, the motion of the particle can be modelled.

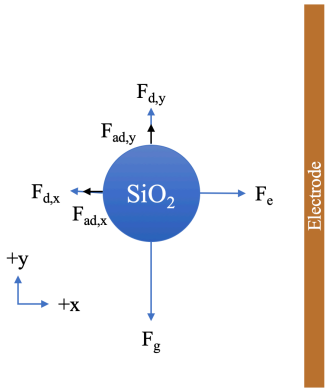

Fig. 4. Force balance acting on the spherical silica particles in the free-fall.

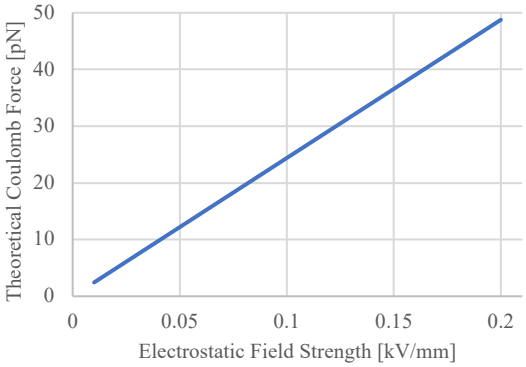

Fig. 5. Theoretical Coulomb force magnitude acting on a single 87 µm spherical silica particle under increasing electrostatic field strengths.

The electrostatic field within the separator is uniform, as the electrodes are identical in size and shape, and are parallel. The magnitude of the electrostatic field is a function of the potential difference between the

electrodes and the distance separating them. Given the dynamic nature of the free-fall separator, a variety of separation distances and electrode voltages can be used to generate identical fields. In theory, a particle with a constant charge should be more strongly influenced by a stronger electrostatic field, as show in Fig. 5.

4. Results and Discussion

Charge measurements were conducted 7 times. The average temperature and relative humidity were measured to be 20.3°C (const.) and 53.4% (const.), respectively. The average charge measured on the samples was found to be +272 pC/g ± 66 pC/g (95% confidence). This is indicative of a need for a more robust and repeatable charging methodology.

Figures 6-8 present the average fraction of material collected at the positive and negative electrodes under the 75-, 150- and 225-mm electrode spacings. Error bars indicating 95% confidence intervals have been included. The average temperature and relative humidity in the lab over the course of experimentation were 21.2°C ± 0.1°C and 59.9% ± 1.2%, respectively.

The results indicate that the relationship between field strength and the proportion of material reporting to a particular electrode does not increase linearly as expected. Furthermore, an optimal operating condition seems to exist at a lower field strength. This indicates that there is an underlying effect that is overriding the contribution of the electrostatic field.

The data sets collected were grouped by both electrode spacing (3 sets, 42 data points per set) and field strength (14 sets, 9 data points per set) for analysis. The electrode spacing sets were analysed using single factor ANOVA. The variances between the points at each field strength were found to be very small; subsequent investigation via the F-test and paired t-test confirmed that all but one configuration (75 mm, 0.04 kV/mm, coinciding with the peak in Fig. 9) were statistically the same. This indicates that there is not an appreciable improvement to the proportion of material reporting to the hopper with a stronger field.

The effect of electrode spacing at each field strength was also evaluated by single factor ANOVA. The analysis again showed that most data points were statistically similar, with a few exceptions. Subsequent paired t-tests were performed between the 75/150, 150/225 and 75/225 spacings. This analysis showed that 9 out of 14 sets were statistically similar for the 75/150 pair, and 11 out of 14 sets were statistically similar for both the 150/225 and 75/225 sets. At one field strength, 0.06 kV/mm, the three spacings were all found to be statistically unique, indicating that there may be a dependency on electrode spacing.

Across the three spacings, the average material collected at the negative electrode were: 69.5% ± 16.6% (75 mm); 62.7% ± 14.2% (150 mm); and, 62.2% ± 10.6% (225 mm). While there is a difference amongst the averages, further data must be collected to reduce uncertainty, improve clarity, and determine whether or not there do exist unique operating parameters.

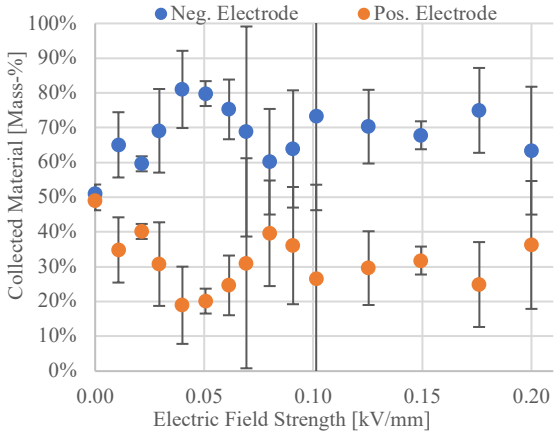

Fig. 6. Mass-% of SiLibeads collected at each electrode with 75-mm spacing relative to electric field strength.

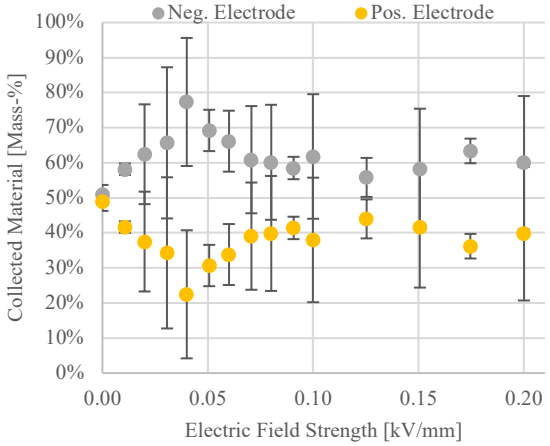

Fig. 7. Mass-% of SiLibeads collected at each electrode with 150-mm spacing relative to electric field strength.

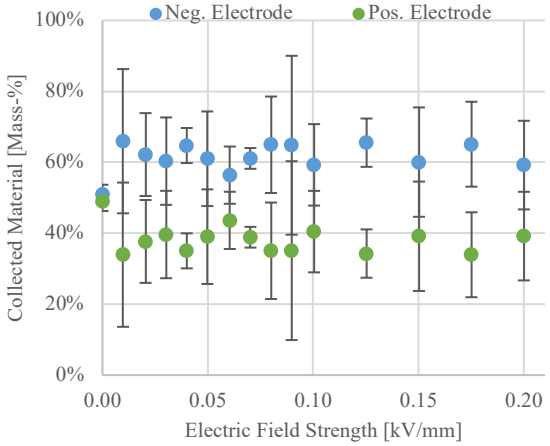

Fig. 8 Mass-% of SiLibeads collected at each electrode with 225-mm spacing relative to electric field strength.

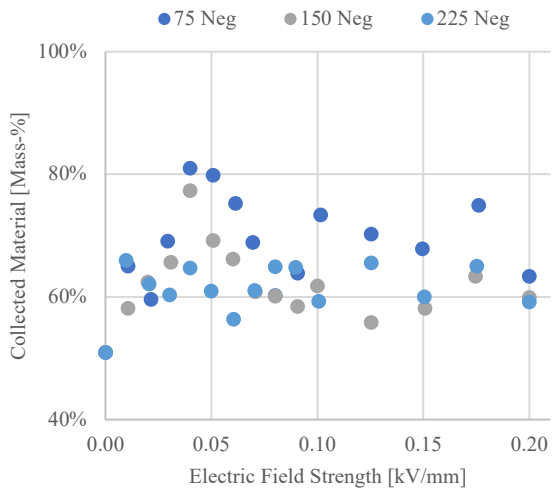

Fig. 9. Comparison of the masses collected from the negative electrode hopper at each of the three electrode spacings.

5. Conclusions

In this work, 10-g samples of 70-110 µm spherical silica SiLibeads were tribocharged and fed into a free-fall electrostatic beneficiation system to measure the effect of electrode spacing and field strength on the quantity of material reporting to a given electrode. The beneficiation system employed three electrode spacings producing a series of increasing, discrete electrostatic fields. The amount of material collected at each electrode was weighed and the proportion of material calculated. The results were grouped and analysed by both electrode separation and field strength, and were analysed using single factor ANOVA, as well as the F- and t-tests to determine the statistical significance.

The statistical analysis of the data has shown that, contrary to the theoretical model, there is no alteration to the operation of the separator by increasing the field strength. All but one data point (75 mm, 0.04 kV/mm) were found to be statistically similar across all field strengths for each electrode spacing. Further, the data sets collected at each field strength across electrode spacings were generally found to be statistically similar, with the exception of 0.06 kV/mm, where each of the three spacing data sets were unique.

Further experimentation is required to reduce uncertainty and to improve the clarity of the data. This will aid in evaluating whether or not the unique points described above are indeed unique, or if they are statistical anomalies.

Acknowledgements

This research has been made possible through the support of the Luxembourg National Research Fund (FNR) under Industrial Fellowship Grant 12489764.

The authors acknowledge the support of the Natural Sciences and Engineering Research Council of Canada (NSERC) [ref: 411291661]. Cette recherche a été financée par le Conseil de recherches en sciences naturelles et en génie du Canada (CRSNG), [réf: 411291661].

References

[1] K. Hadler et al, A universal framework for space resource utilisation (SRU), Planetary and Space Science (2019) [under review].

[2] R. Mueller, P. Van Susante, A review of lunar regolith excavation robotic device prototypes, AIAA SPACE 2011 Conference and Exposition, Long Beach, United States of America, 2011, 27 – 29 September.

[3] L.A. Taylor, W.D. Carrier III, Oxygen production on the Moon: An overview and evaluation, in: J.S. Lewis, M.S. Matthews, M.L. Guerrieri (Eds.), Space Science Series, The University of Arizona Press, Tucson, 1993, pp. 69–108.

[4] K. Lee et al, The ROxygen project: Outpost-scale lunar oxygen production system development at Johnson Space Center, J. Aero. Eng., 26 (2013) 67–73.

[5] A. Muscatello, R. Gustafson, The 2010 field demonstration of the solar carbothermal reduction of regolith to produce oxygen, First Joint Meeting of the Space Resources Roundtable and the Planetary & Terrestrial Mining Sciences Symposium, Golden, United States of America, 2010, June.

[6] S.S. Schreiner, Molten Regolith Electrolysis reactor modeling and optimization of in-situ resource utilization systems (Thesis), MIT Press, Cambridge, 2015.

[7] C.J. Schwandt et al, The production of oxygen and metal from lunar regolith, Planetary and Space Science, 74 (2012) 49–56.

[8] M.A. Gibson, C.W. Knudsen, Apparatus for manufacture of oxygen from lunar ilmenite, US Patent 5,536,378 (July 1996).

[9] D.S. McKay et al, The lunar regolith, in: G.H. Heiken, D.T. Vaniman, B.M. French (Eds.), The Lunar Sourcebook, Cambridge University Press, Cambridge, 1991, pp. 285–356.

[10] W.D. Carrier III, Particle size distribution of lunar soil, J. Geotech. and Geoenv. Eng., 129 (2003) 956–959.

[11] J.J. Cilliers, J.N. Rasera, K. Hadler, Estimating the scale of space resource utilisation (SRU) operations to satisfy lunar oxygen demand, Planetary and Space Science, (2010).

[12] G.R. Ballantyne, P.N. Holtham, Application of dielectrophoresis for the separation of minerals, Minerals Eng., 23 (2010) 350–358.

[13] G.R. Ballantyne, Application of dielectrophoresis to mineral processing (Thesis), The University of Queensland, Brisbane, 2011.

[14] G.R. Ballantyne, P.N. Holtham, Evaluation of the potential for using dielectrophoresis to separate minerals, Minerals Eng., 55 (2014) 75–79.

[15] F. Fraas, Electrostatic separation of granular materials, Bulletin 603, United States Department of the Interior, Bureau of Mines (1962).

[16] S. Trigwell et al, Electrostatic beneficiation of lunar simulant, Internal Report, NASA (2006)

[17] S. Trigwell et al, The use of tribocharging in the electrostatic beneficiation of lunar simulant, IEEE Trans. on Ind. App., 45 (2009) 1060–1067.

[18] S. Trigwell et al, Electrostatic beneficiation of lunar regolith: Applications in in situ resource utilization, J. Aero. Eng., 26 (2012) 30–36.

[19] J.W. Quinn et al, Evaluation of tribocharged electrostatic beneficiation of lunar simulant in lunar gravity, J. Aero. Eng., 26 (2012) 37–42.

[20] J. Captain et al, Tribocharging lunar simulant in vacuum for electrostatic beneficiation, Space Technology and Applications International Forum Albuquerque, United States of America, 2007, 11 – 15 February.

[21] B.A. Wills, J. Finch, Wills' mineral processing technology: An introduction to the practical aspects of ore treatment and recovery, eighth ed., Butterworth-Heinemann, Oxford, 2016.

[22] J.N. Rasera, J.J. Cilliers, K. Hadler, The beneficiation of lunar regolith for space resource utilisation: A review, Planetary and Space Science (2019) [under review].